JOURNAL OF MAGNETIC RESONANCE, Series A 109, 270–272 (1994)

High-Resolution Heteronuclear Dipolar Solid-State NMR Spectroscopy

C. H. WU, A. RAMAMOORTHY, AND S. J. OPELLA

Department of Chemistry, University of Pennsylvania, Philadelphia, Pennsylvania 19104

Received April 28, 1994

By combining polarization inversion (*1*) with flip-flop (*2*) Lee–Goldburg (*3*) homonuclear decoupling on the abundant I spins following spin-lock cross polarization to the dilute S spins during the t_1 interval of a pulse sequence, very high-resolution two-dimensional heteronuclear I–S dipolar spectra of solid samples can be obtained. Linewidths in the dipolar dimension are reduced by more than an order of magnitude compared to a conventional separated-local-field spectrum obtained without homonuclear decoupling during the t_1 interval. The combination of narrow lines and favorable scaling factor has such a dramatic effect on the appearance of the spectra that it is now feasible to formulate solid-state NMR experiments where heteronuclear dipolar couplings rather than chemical shifts provide the fundamental mechanism for resolution among sites. Further, dipolar splittings and chemical-shift frequencies can be used in combination in three-dimensional spectra (*4*) to enhance resolution even further.

The heteronuclear dipole–dipole interaction is generally the dominant factor in determining lineshapes, linewidths, and relaxation parameters in NMR spectra of dilute spin-$\frac{1}{2}$ nuclei in solids. It also determines the kinetics of cross polarization (*5, 6*). Although dipole–dipole interaction was recognized as a significant source of structural information in early NMR experiments (*7*), since the doublets observed in spectra of two spin-$\frac{1}{2}$ nuclei coupled to each other have splittings determined by the distance between the two nuclei and the angle between their internuclear vector and the applied magnetic field, it was not until the development of two-dimensional separated-local-field spectroscopy (*8*) that heteronuclear dipole–dipole couplings could be resolved and characterized in single-crystal (*9*) and oriented (*10*) samples relevant to chemical and biochemical problems. The chemical-shift dimension in separated-local-field spectra has intrinsically high resolution because continuous on-resonance ^{1}H irradiation decouples the heteronuclear dipolar interactions during the t_2 interval when data are acquired; however, even with the use of homonuclear multiple-pulse decoupling (*11*), the doublets (or multiplets) in the dipolar frequency dimension are generally quite broad due to the rapid decay of the S-spin signals from incomplete decoupling of the homonuclear dipole–dipole interactions, short T_2, and cumulative effects of longer-range heteronuclear dipole–dipole interactions. Polarization inversion following spin-lock cross polarization provides an alternative approach to probe and measure heteronuclear dipolar couplings in a variety of applications (*1, 12–17*); however, selectivity is limited by spin diffusion among the abundant I spins under conditions of continuous on-resonance irradiation.

Since our research is focused on solid-state NMR structural studies of proteins (*18*), we utilize the ^{1}H–^{15}N heteronuclear dipole–dipole interaction in amide sites of model peptides for spectroscopic development. The spectra presented in this Communication were obtained on a single-crystal sample of [^{15}N]acetylleucine with four magnetically distinct amide sites. These experiments are equally applicable to ^{1}H–^{13}C or other heteronuclear couplings between two (or several) different spin-$\frac{1}{2}$ nuclei.

Separated-local-field spectroscopy (*8*) elegantly incorporates radiofrequency irradiations in the form of multiple-pulse sequences to average out homonuclear dipole–dipole couplings and double-resonance procedures to average out heteronuclear dipole–dipole couplings. The simplest and most widely used separated-local-field pulse sequence is diagramed in Fig. 1A; it relies on the relatively large magnitude of the heteronuclear dipolar coupling between directly bonded nuclei to overwhelm the effects of homonuclear and longer-range heteronuclear dipolar couplings during the t_1 interval (*19*). The pulse sequence in Fig. 1A is generally successful in associating a defined dipolar coupling with each of the resonances resolved on the basis of their chemical shifts, as shown in the spectrum in Fig. 2A. In the slice taken through half of the symmetric dipolar frequency spectrum shown in Fig. 3A the peak has a linewidth of 5 kHz, more than half the 9 kHz spectral range (the maximum ^{1}H–^{15}N heteronuclear dipolar splitting is 18 kHz). The benefits of applying homonuclear ^{1}H–^{1}H decoupling during the t_1 interval, as the ^{1}H–^{15}N heteronuclear dipolar interaction evolves, are diminished by the substantial scaling associated with most homonuclear line-narrowing procedures. The spectra in Figs. 2B and 3B were obtained with the pulse sequence diagramed in Fig. 1B, where Lee–Goldburg off-resonance decoupling (*3*), which we find to be somewhat more effective than WAHUHA (*11*) or MREV-8 (*20*) pulse sequences in this situation, is applied during the t_1 interval. Although the dipolar linewidth is narrowed to 700 Hz in the

1064-1858/94 $6.00
Copyright © 1994 by Academic Press, Inc.
All rights of reproduction in any form reserved.

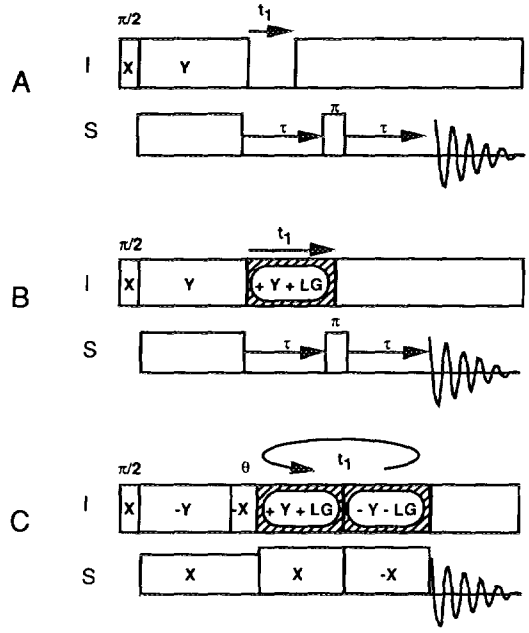

FIG. 1. Pulse sequences for two-dimensional heteronuclear dipolar/chemical-shift spectroscopy. (A) Simplest version of the separated-local-field experiment, (B) separated-local-field experiment with Lee–Goldburg homonuclear decoupling applied during the t_1 period, and (C) PISEMA experiment. Y+LG indicates a Y radiofrequency phase and a positive frequency jump satisfying the Lee–Goldburg condition. The spin lock during the t_1 period is Y+LG and −Y−LG, respectively, for the first and second halves of each cycle. Each t_1 increment corresponds to an integral number of cycles defined by the flip-flop Lee–Goldburg sequence.

spectrum in Fig. 2B, the effective dipolar spectral range is reduced to less than 5 kHz by scaling. The improvement in resolution from the addition of homonuclear decoupling during the t_1 interval shown in Figs. 2B and 3B is among the best we have observed; more typically, after taking scaling into account there is only marginal improvement in resolution.

The pulse sequence diagramed in Fig. 1C gives the spectrum in Fig. 2C with dipolar linewidths of 200 Hz, as shown in Fig. 3C, which are more than an order of magnitude narrower than those in Fig. 3A and substantially narrower than those in Fig. 3B. The scaling factor of 0.82 for this pulse sequence gives a spectral range for the spectrum in Fig. 2C nearly twice that in Fig. 2B. The combination of substantial line narrowing and minimal scaling results in a striking improvement in the resolution of the spectrum in Fig. 2C over that in Fig. 2A.

We call the pulse sequence diagramed in Fig. 1C PISEMA, an acronym for *p*olarization *i*nversion *s*pin *e*xchange at the *m*agic *a*ngle. Following a conventional spin-lock cross polarization from the abundant I-spin magnetization to the dilute S spins, a flip-flop Lee–Goldburg (phase- and frequency-shifted) pulse sequence (*2, 21*) is used to spin-lock the I spins along the magic angle. The spin-lock field applied to the S spins is phase alternated synchronously with the flip-flop Lee–Goldburg procedure to enable coherent transfer of magnetization by cross polarization. The application of the flip-flop Lee–Goldburg sequence greatly extends the oscillation time of the S-spin magnetization as it seeks to regain equilibrium with the I-spin magnetization through the phase reversals. However, without polarization inversion of the I spins these oscillations are accompanied by an asymptotic approach to equilibrium, which results in a substantial zero-frequency distortion in the frequency domain of the resulting dipolar spectrum. The polarization inversion during the preparation period brings the abundant I spins to negative spin temperature before the magnetization is allowed to exchange under the influence of the heteronuclear dipolar couplings, since cross polarization brings the I and S spins to

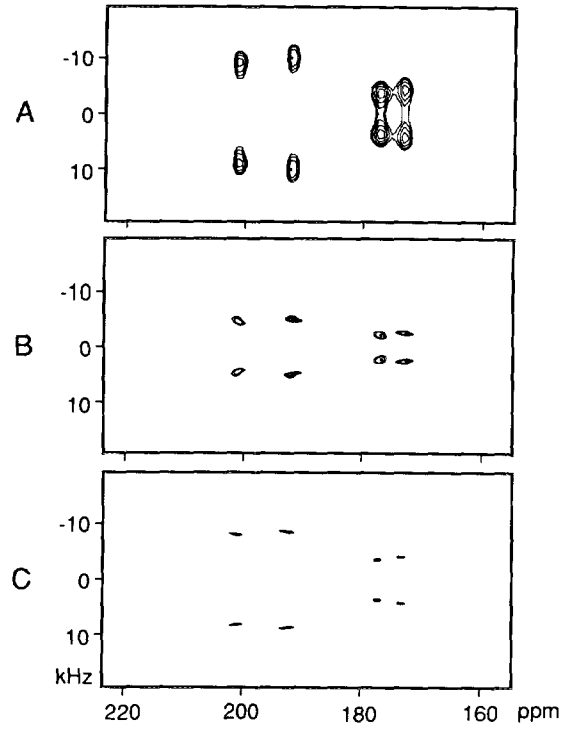

FIG. 2. Two-dimensional spectra obtained using the pulse sequences diagrammed in Fig. 1 on a 28 mg single crystal of an arbitrary orientation of [^{15}N]acetylleucine at room temperature on a homebuilt four-channel spectrometer with a 12.9T wide-bore Magnex 550/89 magnet. [^{15}N]Acetylleucine was prepared by acetylating (99% enriched) L-[^{15}N]leucine (Isotec, Inc.) with acetic anhydride in a saturated NaOH solution. The single crystal was grown from saturated aqueous solutions. The ^{1}H and ^{15}N resonance frequencies are, respectively, 550 and 55.7 MHz. Spectra A, B, and C correspond to pulse sequences A, B, and C in Fig. 1 and resulted from eight transients acquired for 32, 64, and 128 t_1 increments, respectively; t_1 was incremented in A, B, and C by 21.2, 39.2, and 39.2 μs, respectively, corresponding to spectral widths of 47.17, 50.02, and 31.10 kHz after scaling by the experimental factors of 1, 0.51, and 0.82. All three experiments used a cross-polarization period of 1 ms and a recycle delay of 10 s. Radiofrequency field strengths of about 83 kHz were used for both ^{1}H and ^{15}N irradiations, dictating frequency jumps of 58.9 kHz to meet the Lee–Goldburg condition. The ^{15}N radiofrequency field strength during the spin lock was increased to match the effective ^{1}H radiofrequency field strength.

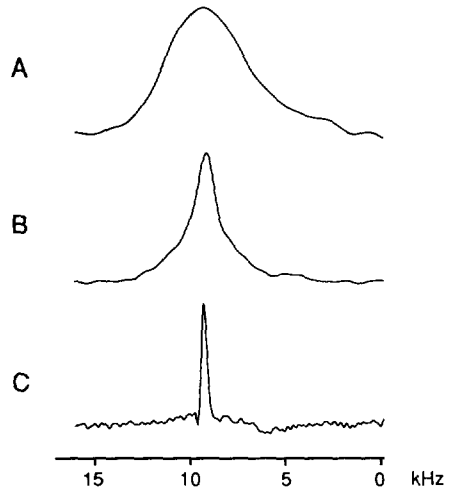

FIG. 3. One-dimensional slices along the dipolar frequency axis in the spectra in Fig. 2 taken at 196 ppm on the ^{15}N chemical-shift axis. The spectra are scaled by 1, 0.51, and 0.82 for A, B, and C, respectively, enabling the linewidths to be compared directly.

the same spin temperature prior to the 180° phase shift of the spin-lock field for the I spins.

The S-spin magnetization transferred from the I-spin reservoir before the polarization inversion has a negligible effect on I-spin temperature. Since the total magnetization participating in spin exchange is twice that without polarization inversion, increased sensitivity is a bonus with this pulse sequence. After the I–S contact is established, the nuclei exchange magnetization due to the spin-temperature imbalance with a frequency determined by the magnitude of the heteronuclear dipolar coupling. The oscillations during the t_1 interval continue for a long time because spin diffusion among the abundant I spins is suppressed by the flip-flop Lee–Goldburg sequence and the relaxation is governed by $T_{1\rho}$ processes in the tilted rotating frame rather than T_2.

In the spectrum in Fig. 3C the ratio of spectral range to linewidth is 36, which is substantially better than the ratios of about 2 and 7 in the spectra in Figs. 3A and 3B, respectively, and comparable to the ratios observed in the chemical-shift dimension, where the linewidths are typically 2–4 ppm and the spectral range due to the ^{15}N amide chemical-shift tensor is 170 ppm. This indicates that it is feasible to distinguish among molecular sites on the basis of small variations in their heteronuclear dipole–dipole couplings resulting from differences in bond lengths or orientations of the bonds with respect to the applied magnetic field in both two- and three-dimensional spectra (*4*). It also makes very precise measurements of these couplings available for analysis of structural parameters.

PISEMA is notable because the signals decay during the t_1 interval according to $T_{1\rho}$, which is typically much longer than T_2, sensitivity is enhanced, and the scaling factor is very favorable. PISEMA (and related sequences) have the potential to go beyond heteronuclear dipolar spectroscopy, since it can be applied in any mixing period that requires selectivity. For example, it improves the selectivity of dipolar coherence transfer from I to S nuclei when used as a mixing period in multidimensional heteronuclear correlation experiments (*22–24*). The benefits of PISEMA are also realized with uniaxially oriented samples as well as polycrystalline samples in the presence and absence of magic-angle sample spinning.

ACKNOWLEDGMENTS

We thank M. T. Melchior for sending us a copy of his original 1981 ENC poster. This research was supported by Grants GM29754 and GM24266 from the National Institutes of Health. It utilized the Resource for Solid-State NMR of Proteins at the University of Pennsylvania, which is supported by Grant RR09731 from the Biomedical Research Technology Program, Division of Research Resources, National Institutes of Health.

REFERENCES

1. M. T. Melchior, Poster and Abstract, 21st Experimental NMR Conference, 1981.
2. M. Mehring and J. S. Waugh, *Phys. Rev. B* **5,** 3459 (1972).
3. M. Lee and W. I. Goldburg, *Phys. Rev. A* **140,** 1261 (1965).
4. B. S. Arun Kumar and S. J. Opella, *J. Magn. Reson. A* **101,** 333 (1993).
5. L. Muller, A. Kumar, T. Baumann, and R. R. Ernst, *Phys. Rev. Lett.* **32,** 1402 (1974).
6. R. K. Hester, J. L. Ackerman, V. R. Cross, and J. S. Waugh, *Phys. Rev. Lett.* **34,** 993 (1975).
7. G. E. Pake, *J. Chem. Phys.* **16,** 327 (1948).
8. J. S. Waugh, *Proc. Natl. Acad. Sci. USA* **73,** 1394 (1976).
9. R. K. Hester, J. L. Ackerman, B. L. Neff, and J. S. Waugh, *Phys. Rev. Lett.* **36,** 1081 (1976).
10. S. J. Opella and J. S. Waugh, *J. Chem. Phys.* **66,** 4919 (1977).
11. J. S. Waugh, L. M. Huber, and U. Haeberlen, *Phys. Rev. Lett.* **20,** 180 (1968).
12. N. Zumbulyadis, *J. Chem. Phys.* **86,** 1162 (1987).
13. D. G. Cory and W. M. Ritchey, *Macromolecules* **22,** 1611 (1989).
14. P. Tekely and J. J. Delpuech, *Fuel* **68,** 947 (1989).
15. P. Tekely, F. Montigny, D. Canet, and J. J. Delpuech, *Chem. Phys. Lett.* **175,** 401 (1990).
16. P. Palmas, P. Tekely, and D. Canet, *J. Magn. Reson. A* **104,** 26 (1993).
17. W. Xiaoling, Z. Shanmin, and W. Xuewen, *J. Magn. Reson.* **77,** 343 (1988).
18. S. J. Opella, P. L. Stewart, and K. G. Valentine, *Q. Rev. Biophys.* **19,** 7 (1987).
19. E. F. Rybaczewski, B. L. Neff, J. S. Waugh, and J. S. Sherfinski, *J. Chem. Phys.* **67,** 1231 (1977).
20. W. K. Rhim, D. D. Elleman, and R. W. Vaughan, *J. Chem. Phys.* **58,** 1772 (1973).
21. A. Bielecki, A. C. Kolbert, H. J. M. de Groot, R. G. Griffin, and M. H. Levitt, *Adv. Magn. Reson.* **14,** 111 (1990).
22. P. Caravatti, G. Bodenhausen, and R. R. Ernst, *Chem. Phys. Lett.* **89,** 363 (1982).
23. J. Roberts, S. Vega, and R. G. Griffin, *J. Am. Chem. Soc.* **106,** 2506 (1984).
24. B. S. Arun Kumar and S. J. Opella, *J. Magn. Reson. A* **95,** 417 (1991).